Journal of Environmental Protection, 2025, 16(11), 1113-1128
https://www.scirp.org/journal/jep
ISSN Online: 2152-2219
ISSN Print: 2152-2197

Adsorption of Congo Red in Aqueous Solution on Activated Carbon Prepared from the Bark of the Asparagus Palm (*Laccosperma robustum*)

Adam Bouraïma*, Albert Novy Messi Me Ndong, Crislain Bissielou, Phil Lewis Mpampoungou Langama, Jean-Jacques Anguile

Laboratoire de Chimie des Matériaux inorganiques, Département de Chimie, Faculté des Sciences, Université des Sciences et Techniques de Masuku, Franceville, Gabon
Email: *abourae@yahoo.fr

How to cite this paper: Bouraïma, A., Ndong, A.N.M.M., Bissielou, C., Langama, P.L.M. and Anguile, J.-J. (2025) Adsorption of Congo Red in Aqueous Solution on Activated Carbon Prepared from the Bark of the Asparagus Palm (*Laccosperma robustum*). *Journal of Environmental Protection*, **16**, 1113-1128.
https://doi.org/10.4236/jep.2025.1611059

Received: September 24, 2025
Accepted: November 4, 2025
Published: November 7, 2025

Abstract

This study focused on the adsorption of Congo Red (CR) in aqueous solution by activated carbons (AC) prepared from the bark of the asparagus palm (*Laccosperma robustum*) through chemical activation with phosphoric acid (H_3PO_4) and potassium hydroxide (KOH). The experiments were carried out in batch mode. Adsorption parameters such as stirring time, AC mass, solution pH, and initial RC concentration were studied. The adsorption isotherm and kinetics were also studied. This study showed that the optimal adsorption conditions were 15 and 25 minutes for CAK and CAP stirring times, respectively, a mass of 0.05 g, and a pH of 2 for both CA. The maximum RC adsorption quantities were 34.34 mg/g for CAP and 38.90 mg/g for CAK for a concentration of 100 mg/L each. The Freundlich and Temkin isotherms best describe the RC adsorption process on CAP and CAK. The pseudo-first-order, pseudo-second-order, and Elovich kinetic models best describe the adsorption kinetics of CR on PAC. Meanwhile, the pseudo-second-order and Elovich models best describe the adsorption kinetics of CR on PAC. The results obtained showed that activated carbons were effective for the adsorption of CR in aqueous solution.

Keywords

Adsorption, Congo Red, Activated Carbon, *Laccosperma robustum*

1. Introduction

Industrial activities have contributed to the development of several countries but

have also generated various types of pollution [1]. The water sector has been severely affected by the discharge of industrial effluents into the environment, leading to pollution by dyes and heavy metals [2]. Numerous cases of river pollution have been recorded in Gabon. These include: the Mikouagna and Moundjai rivers in the province of Haut-Ogooué [3], the Irougou, Obsugue, and Dubanga rivers in the province of Ngounié, causing changes in water color, vegetation degradation, foul odors emanating from the river, and fish deaths [4] [5]. Congo Red (CR) is an acid dye belonging to the azo class. It was used to dye textiles but is now used in histology and mycology [6]. Prolonged exposure to this dye causes allergic reactions, skin cancer, and bladder cancer [6]. According to the Danish Environmental Protection Agency, cancer risk estimates require setting a limit concentration of 3.1 µg/L for azo dyes in drinking water [7]. Consequently, decontamination of water polluted by these chemical compounds is necessary for both human health and environmental protection. As a result, several types of treatment have been proposed, including reverse osmosis, membrane separation, ion exchange, coagulation-flocculation, electrochemistry, chemical oxidation, and adsorption [8]. Of all these separation processes, adsorption is often used because it is an easily achievable, inexpensive, and above all effective method for removing pollutants even at low concentrations [8]. Activated carbon (AC) is the most widely used adsorbent in the purification or separation of liquids and gases due to its very large specific surface area [9]. The main objective of this work is the adsorption of RC in aqueous solution by CA prepared from the bark of the asparagus palm (*Laccosperma robustum*) through chemical activation with phosphoric acid and potassium hydroxide. To this end, the effect of parameters such as stirring time, solution pH, adsorbent mass, and initial concentration was studied in order to find the ideal conditions for removing this dye from aqueous solution. Similarly, studies on the isotherm and adsorption kinetics were carried out to see which ones best describe the adsorption mechanism.

2. Materials and Methods

2.1. Materials

2.1.1. Congo Red

CR is an acid dye belonging to the azo class, with the chemical formula $C_{32}H_{22}N_6O_6Na_2S_2$ and a molar mass of 650.06 g/mol. The structure of CR is shown in Figure 1 below:

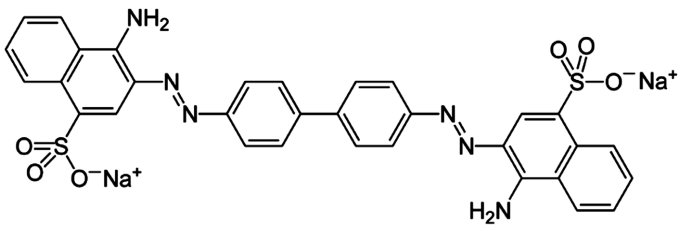

Figure 1. Structure of the Congo Red molecule.

A stock solution of RC with a concentration of 500 mg/L was prepared by weighing 0.5 g of RC powder and placing it in a 1000 mL volumetric flask filled to ¾ capacity with distilled water. The resulting solution was homogenized for 1 hour and then topped up with distilled water to the mark. Daughter solutions with concentrations of 50, 60, 70, 80, 90, and 100 mg/L were prepared by successive dilution of the stock solution in 100 mL volumetric flasks.

2.1.2. Activated Carbons

The ACs used in this work were prepared and characterized by Langama & *al.* [10]. **Table 1** below presents some characteristics of these ACs.

Table 1. Some characteristics of CAs [10].

Settings	Adsorbents	
	CAP	CAK
Iodine index (mg/g)	850.56	865.49
pH_{PCN}	4.4	7
Carboxylic acids (mmol/g)	0.625	0.625
Lactones (mmol/g)	0.5625	0.0625
Phenolics (mmol/g)	1.5625	1.5625
Total Acid (mmol/g)	2.75	2.25
Total Base (mmol/g)	1	2.25

2.2. Methods

2.2.1. Adsorption of Congo Red in Aqueous Solution in Batch Mode

The adsorption of CR was carried out at room temperature by bringing different masses of activated carbon (0.05, 0.06, 0.07, 0.08, 0.09, and 1 g) in 20 mL of the solution at different pH levels (2, 3, 4, 5, 6, 7, 8, and 9) and different concentrations (50, 60, 70, 80, 90, and 100 mg/L). The mixtures were stirred for different periods of time (5, 10, 15, 20, 25, 30, 35, 40, 45, 50, 55, 60, 70, and 80 minutes). After stirring, the mixtures were filtered using filter paper and the filtrates obtained were measured using a UV-visible spectrophotometer at a maximum wavelength of 476 nm. The amount of RC adsorbed at equilibrium (Q_e) was calculated using Equation (1):

$$Q_e = \frac{(C_o - C_e) \times V}{m} \quad (1)$$

where,

Q_e (mg/g): amount of solute adsorbed at equilibrium,

C_o (mg/L): initial concentration of solute,

C_e (mg/L): concentration of adsorbate at equilibrium,

V (L): volume of solution,

m (g): mass of adsorbent.

The initial pH of the Congo red solutions was measured using a pH meter and adjusted using hydrochloric acid (HCl) or sodium hydroxide (NaOH) solutions, both with a normality of 0.1 N. The stirring speed was kept constant (500 rpm) for all adsorption experiments. The parameters that were varied were the initial pH of the solution, the contact time, the mass of activated carbon, and the initial concentration of the solute in solution.

2.2.2. Study of the Isotherm and Adsorption Kinetics

The different nonlinear forms of the Langmuir, Freundlich, Dubinin-Kaganer-Raduskevich (D-K-R), and Temkin isotherm models used in this work are shown in Table 2 below:

Table 2. Isotherm models.

Modèles d'isothermes	Equations
Langmuir	$Q_e = \frac{Q_m K_L C_e}{1 + K_L C_e}$ (2)
Freundlich	$Q_e = k_F C_e^{1/n}$ (3)
Temkin	$Q_e = \frac{RT}{b_T} \ln\left(A_T C_e\right)$ (4)
D-K-R	$Q_e = Q_s \exp\left(-\beta\varepsilon^2\right)$ (5)

where,

Q_e (mg/g): amount of solute adsorbed at equilibrium,

Q_m (mg/g): maximum amount of solute adsorbed,

C_e (mg/L): residual concentration of solute at equilibrium in the solution,

K_L (L/mg): Langmuir constant related to adsorption energy,

K_F ($mg^{1-1/n} \cdot L^{1/n} \cdot g^{-1}$): Freundlich constant,

n: Freundlich coefficient,

A_T (L/mg): Temkin constant,

b_T (J/mol): constant related to adsorption heat,

R (8.314 J/K/mol): ideal gas constant,

T (K): absolute temperature,

β (mol^2/J^2): constant related to adsorption energy,

ε: Polanyi potential given by

$$\varepsilon = RT \ln\left(1 + \frac{1}{c_e}\right) \quad (6)$$

This study was conducted using various models, the nonlinear forms of which are presented in Table 3 below.

Table 3. Kinetics models.

Models Kinetics	Equations
Pseudo-first order	$Q_t = Q_e\left(1-\mathrm{e}^{K_1 t}\right)$ (7)
Pseudo-second order	$Q_t = \dfrac{Q_e^2 K_2 t}{1+Q_e K_2 t}$ (8)
Elovich	$Q_t = \dfrac{1}{\beta}\ln\left(\alpha\beta t+1\right)$ (9)
Intra-particle diffusion	$Q_t = k_{dif} t^{1/2} + C_o$ (10)

where,

Q_t (mg/g): amount of solute adsorbed at time t,

Q_e (mg/g): amount of solute adsorbed at equilibrium,

K_1 (min^{-1}): pseudo-first-order adsorption rate constant,

K_2 (g/mg/min): pseudo-second-order adsorption rate constant,

α (mg/g/min): initial adsorption rate,

β (g/mg): desorption constant,

K_{dif} (mg/g/min1/2): intra-particle diffusion rate constant,

C (mg/L): originally ordered.

Nonlinear regression was applied using the Solver function in Microsoft Excel 2016. The best fit of the experimental results was evaluated using the correlation coefficient (R^2), the root mean square error (RMSE), and the nonlinear chi-square test (χ^2). A high R^2 value (or low RMSE and χ^2 values) gives the best fit and similarity between the model and the experimental data. The respective calculation formulas for R^2, RMSE, and χ^2 are as shown in Equations (11)-(13) below:

$$R^2 = 1-\frac{\sum_{n=1}^{n}\left(Q_{e.exp,n}-Q_{e.pre,n}\right)^2}{\sum_{n=1}^{n}\left(Q_{e.exp,n}-\overline{Q_{e.exp,n}}\right)^2} \quad (11)$$

$$\chi^2 = \sum_{n=1}^{n}\frac{\left(Q_{e.exp,n}-Q_{e.pre,n}\right)^2}{Q_{e.exp,n}} \quad (12)$$

$$\mathrm{RMSE} = \sqrt{\frac{\sum_{n=1}^{n}\left(Q_{e.exp,n}-Q_{e.pre,n}\right)^2}{n-1}} \quad (13)$$

$Q_{e.exp}$ (mg/g): experimental equilibrium adsorption amount,

$Q_{e.pre}$ (mg/g): predicted (theoretical) adsorption amount,

$Q_{e.exp}$ (mg/g): average experimental equilibrium adsorption amount.

3. Results and Discussion

3.1. Calibration Line

The determination of the absorbances of the RC solutions at different concentrations at λ_{max} = 476 nm enabled the calibration curve shown in **Figure 2** below to be plotted:

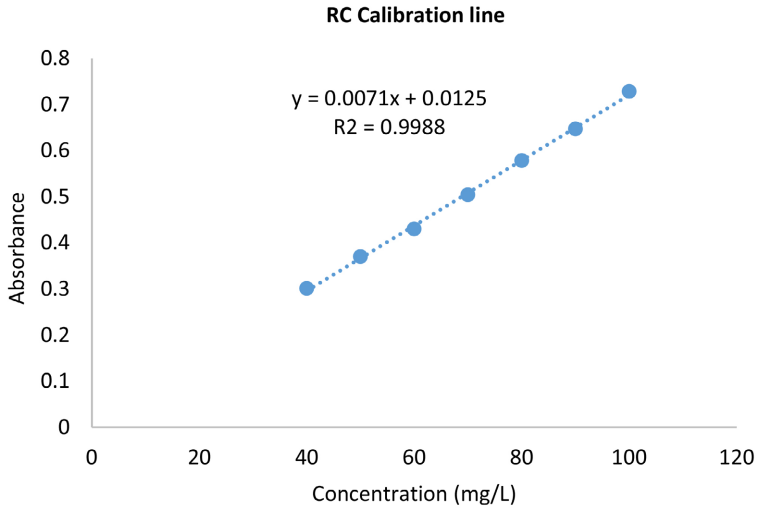

Figure 2. RC calibration line.

The correlation coefficient R^2 = 0.9988 indicates that approximately 99.88% of the prepared daughter solutions lie on the calibration curve.

3.2. Influence of the pH of the RC Solution

The influence of pH was determined by varying the pH from 2 to 9 with a mass of 0.05 g of CA, an initial concentration of 100 mg/L, and a stirring time of 30 minutes. The results obtained are shown in **Figure 3** below:

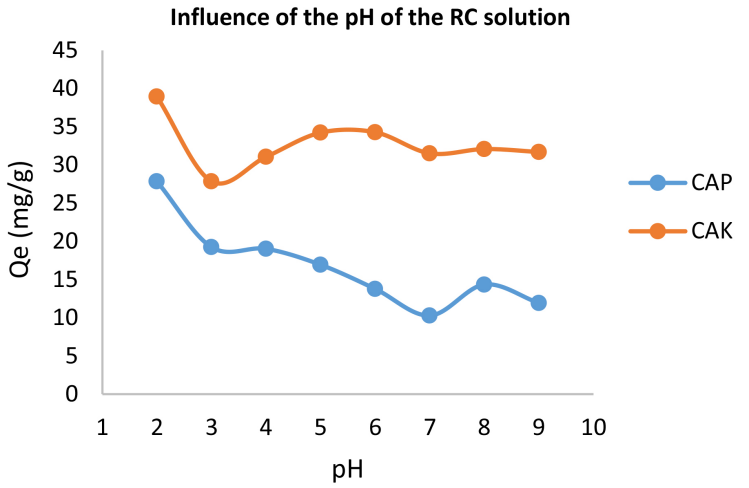

Figure 3. Influence of the pH of the RC solution.

The results in **Figure 3** show that the amount of adsorbed RC molecules decreases from 27.859 to 11.915 mg/g for CAP and from 38.957 to 31.690 mg/g for CAK as the pH increases from 2 to 11. The adsorption of molecules in an acidic environment is thought to be due to electrostatic interaction forces between positively charged CAs and anionic RC [11]. CAP is positively charged due to its pKa of 4.4, while that of CAK is 7 and RC molecules are negatively charged. There

would be protonation of the two primary amines (-NH_2) attached to the two naphthalene rings located at both ends of the RC molecules [12]. The decrease in the amount of RC molecules adsorbed would be due to electrostatic repulsion between the RC on the negatively charged CA [11] [12]. Indeed, an increase in pH leads to an increase in negatively charged sites. There would then be competition between OH- ions and RC molecules. Similar results have been obtained by other researchers [13] [14]. Consequently, pH 2 was chosen as the optimal pH for the subsequent experiments.

3.3. Influence of Contact Time

The stirring time was varied from 5 to 60 minutes using a solution of RC at a concentration of 100 mg/L, at pH = 2 and a mass of 0.05 g of CA. The results are shown in **Figure 4** below:

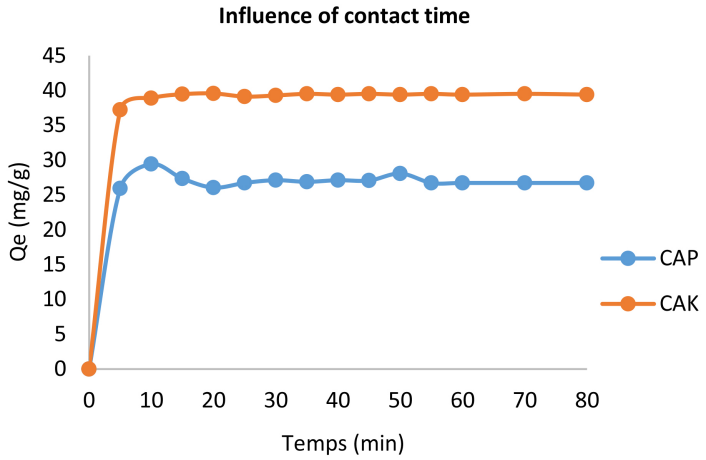

Figure 4. Influence of contact time.

Figure 4 shows that RC adsorption is rapid during the first 5 minutes for activated carbons, then slows down to reach equilibrium at 15 minutes for CAK and 25 minutes for CAP. The rapidity of RC adsorption in the first 5 minutes is thought to be due to the availability of free adsorption sites on the surface of activated carbons [15]. Once the first CR molecules have bound to the surface of the activated carbons, they clog the pores, preventing the remaining CR molecules in solution from penetrating them. This explains the decrease in the adsorption rate [15]. The maximum amounts of RC adsorbed were 26.732 mg/g for CAP at an equilibrium time of 25 minutes and 39.465 mg/g for CAK at an equilibrium time of 15 minutes.

3.4. Influence of Activated Carbon Mass

The influence of activated carbon mass was determined by varying the mass between 0.05 and 0.1 g during equilibrium times of 15 minutes for CAK and 25 minutes for CAP, at a concentration of 100 mg/g at pH 2. The results obtained are shown in **Figure 5** below:

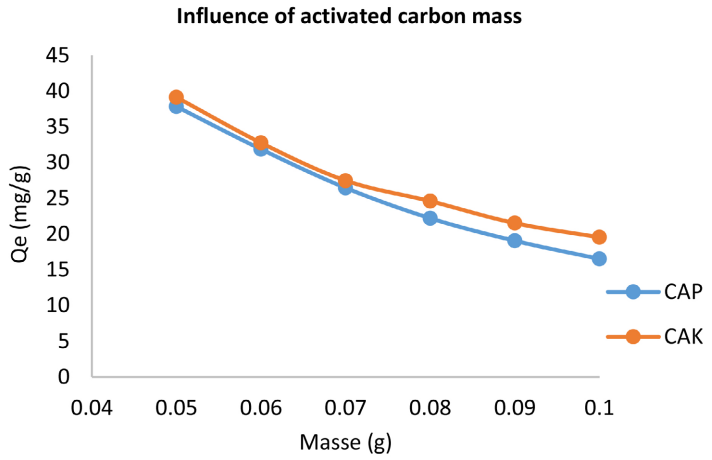

Figure 5. Influence of activated carbon mass.

Figure 5 shows that increasing the mass of CA from 0.05 g to 0.1 g decreases the amount of adsorbed RC molecules from 37.830 mg/g to 16.521 mg/g for CAP and from 39.126 mg/g to 19.535 mg/g for CAK. This decrease may be due to the aggregation of the additional amount of CA [6]. Indeed, the agglomeration of CA particles forms flocs or aggregates that make it difficult for RC molecules to access the adsorption sites and lead to an increase in the distance to be traveled.

3.5. Influence of the Initial Concentration of RC

The influence of the initial concentration of RC was determined by varying the concentration between 50 and 100 mg/L during equilibrium times of 15 minutes for CAK and 25 minutes for CAP, for a mass of 0.05 g of CA and at the optimal pH of 2. The results obtained are shown in **Figure 6** below:

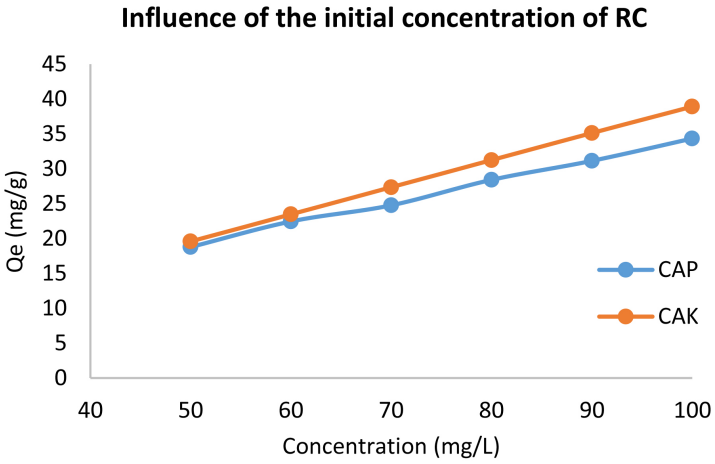

Figure 6. Influence of the initial concentration of RC.

Figure 6 shows that increasing the initial CR concentration from 50 to 100 mg/L increases the amount of adsorbed CR molecules from 18.788 to 34.338 mg/g for CAP and from 19.577 to 38.901 mg/g for CAK. This increase could be ex-

plained by the fact that increasing the initial concentration of RC leads to an increase in collisions between RC molecules and adsorption sites on the surface of activated carbon [15]. Indeed, the reduction in the distance between the RC molecules and the adsorption sites leads to rapid access of the RC molecules to these adsorption sites [15]. Similar results have been obtained by other researchers [16] [17].

3.6. Study of Adsorption Isotherms

The study of adsorption isotherms was carried out using the Langmuir, Freundlich, Temkin, and Dubinin-Kaganer-Raduskevich models, whose nonlinear plots are shown in **Figure 7** below:

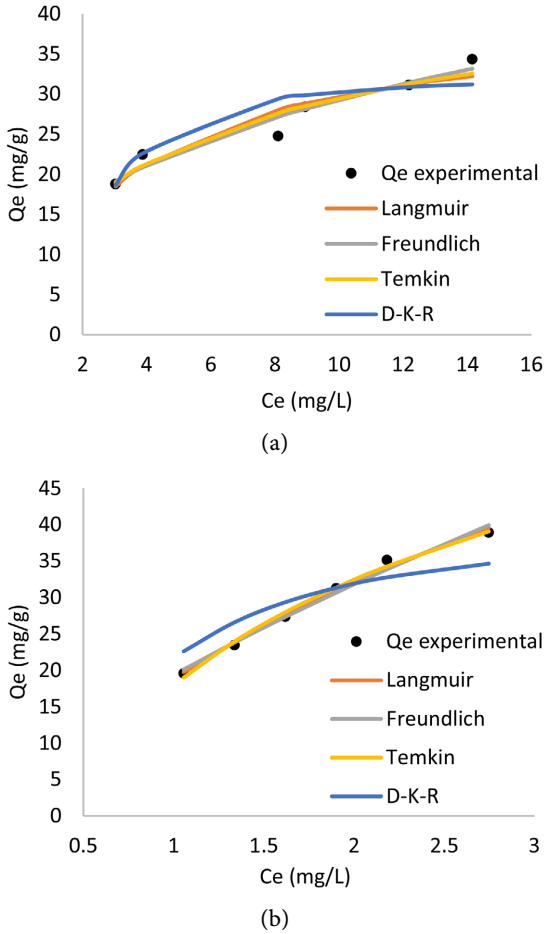

Figure 7. Nonlinear isotherm models for CAP (a) and CAK (b).

The parameters and adjustment coefficients for the RC adsorption isotherms on ACs are summarized in **Table 4** below.

The results in **Table 4** show that the Langmuir isotherm would not be appropriate for describing the adsorption of RC on activated carbon due to the difference between the calculated Q_e value and the experimental Q_e value. The experimental Q_e value is very different from the calculated value.

Table 4. Parameters of the nonlinear isotherm model.

Isotherm models	Parameters	Adsorbents	
		CAP	CAK
Langmuir	Q_e (mg/g) calculated	40.392	106.280
	Q_e (mg/g) experimental	34.338	38.901
	K_L (L/mg)	0.278	0.216
	R^2	0.894	0.992
	RMSE	1.863	0.614
	χ^2	0.660	0.969
	$R_L \times 10^{-3}$	2.980	3.841
Freundlich	K_F ($mg^{1-1/n}.L^{1/n}.g^{-1}$)	12.846	19.334
	$1/n$	0.358	0.717
	R^2	0.940	0.987
	RMSE	1.409	0.824
	χ^2	0.396	0.103
Temkin	A_T (L/mg)	2.768	2.339
	b_T (J/mol)	279.005	117.939
	R^2	0.92	0.993
	RMSE	1.625	0.597
	χ^2	0.506	0.065
D-K-R	Q_s (mg/g)	32.195	39
	B (mol^2/J^2)	1.09×10^{-6}	2×10^{-7}
	E (kJ/mol)	0.677	1.58
	R^2	0.797	0.821
	RMSE	2.589	3.063
	χ^2	1.232	1.667

The Freundlich isotherm would be appropriate for describing the adsorption of RC on activated carbons due to their correlation coefficients R^2 close to unity. In addition, the surface area of activated carbons would be heterogeneous due to values of $(1/n)$ that would be less than unity. These results are similar to the work of other authors [18] [19].

The Temkin isotherm would be appropriate for describing the adsorption of RC on activated carbons due to the correlation coefficient R^2 values of activated carbons being close to unity. Furthermore, b_T values below 8 kJ/mol could indicate the presence of physisorption during the adsorption of RC on activated carbons.

The D-K-R isotherm would not be appropriate for describing the adsorption of RC on activated carbons because its correlation coefficient R^2 is very far from

unity. Nevertheless, it provides information indicating that physisorption could dominate the adsorption mechanism of RC on activated carbons due to E values that are less than 8 kJ/mol.

3.7. Kinetic Study of Adsorption

The nonlinear curves of the pseudo-first-order, pseudo-second-order, Elovich, and intra-particle diffusion models are shown in Figure 8 below:

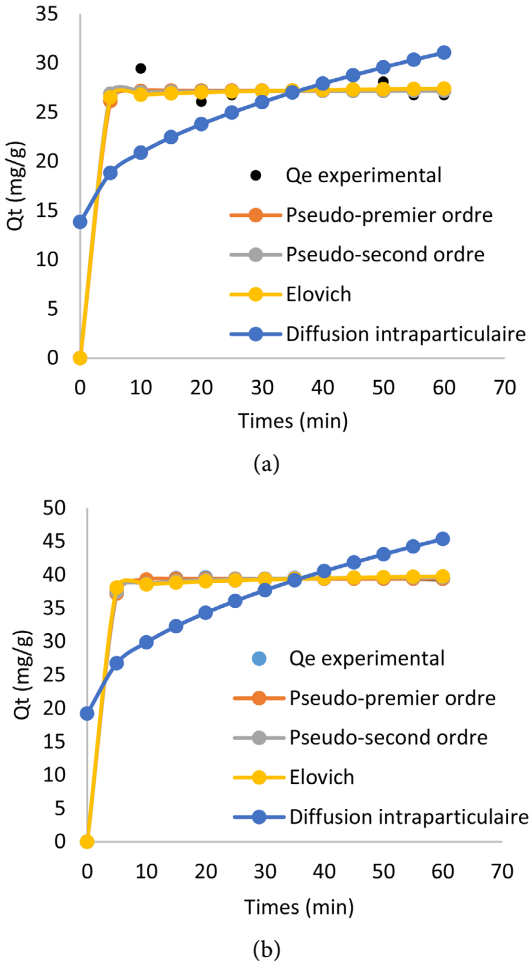

Figure 8. Nonlinear model plots of the adsorption kinetics of CAP (a) and CAK (b).

The parameters and adjustment coefficients for the kinetic models of RC adsorption on CA are summarized in Table 5 below.

The results in Table 5 show that the pseudo-first-order kinetic model would be appropriate for describing the adsorption kinetics of RC on CAP because its correlation coefficient R^2 is close to unity. In addition, the calculated Q_e values and those obtained experimentally would be fairly close. However, the pseudo-first-order kinetic model would not be appropriate for describing the adsorption kinetics of RC on CAK because the experimental Q_e value is higher than the calculated Q_e value, despite its correlation coefficient R^2 being close to unity.

Table 5. Parameters of the nonlinear kinetic model.

Kinetic model	Parameters	Adsorbents	
		CAP	CAK
Pseudo-first order	Q_e calculé (mg/g)	27.202	39.393
	Q_e expérimental (mg/g)	26.732	39.465
	K_1 (min^{-1})	0.646	0.575
	R^2	0.988	0.999
	RMSE	0.859	0.167
	χ^2	0.286	0.078
Pseudo-second order	Q_e calculé (mg/g)	28.806	39.811
	Q_e expérimental (mg/g)	26.732	39.465
	K_2 (mg/g/min)	0.618	0.081
	R^2	0.986	0.999
	RMSE	0.919	0.241
	χ^2	0.328	0.016
Elovich	α (mg/g/min)	5.44×10^{31}	3.83×10^{23}
	β (g/min)	2.856	1.478
	R^2	0.985	0.983
	RMSE	0.966	0.401
	χ^2	0.359	0.047
Intra-particle diffusion	K_{dif}	2.222	3.374
	C_o (mg/g)	13.843	19.205
	R^2	0.438	0.487
	RMSE	9	8.139
	χ^2	7.08	9.319

The pseudo-second-order kinetic model would also be appropriate for describing the adsorption kinetics of RC on activated carbons due to its correlation coefficient R^2 being close to unity. In addition, the calculated Q_e values are higher than or close to the experimental Q_e values. These results are similar to the work of other authors [8] [18] [20].

The Elovich kinetic model would be appropriate for describing the adsorption kinetics of RC on activated carbons due to their correlation coefficients R^2 close to unity, and the values of α being higher than those of β could indicate that the adsorption process occurs by chemisorption on energetically heterogeneous surfaces. All of this could confirm the presence of competition between physisorption and chemisorption in the adsorption process.

Of all the kinetic adsorption models, the intra-particle diffusion model is the

least appropriate for describing the kinetics of RC adsorption on activated carbons due to the low values of the correlation coefficient R^2. Nevertheless, the high Co values could indicate that intra-particle diffusion is not the only step controlling the RC adsorption process on activated carbons.

3.8. Fourier Transform Infrared Spectroscopy (FTIR) of Activated Carbons before and after Adsorption of RC in Aqueous Solution

The IRTF spectra of CAP and CAK before and after adsorption are shown in Figure 9, respectively.

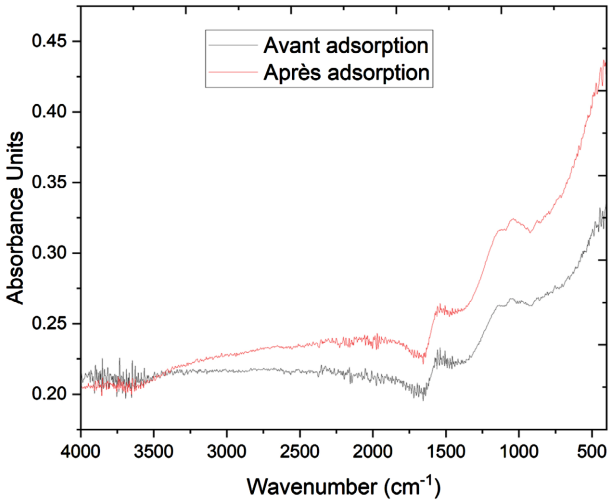

(a)

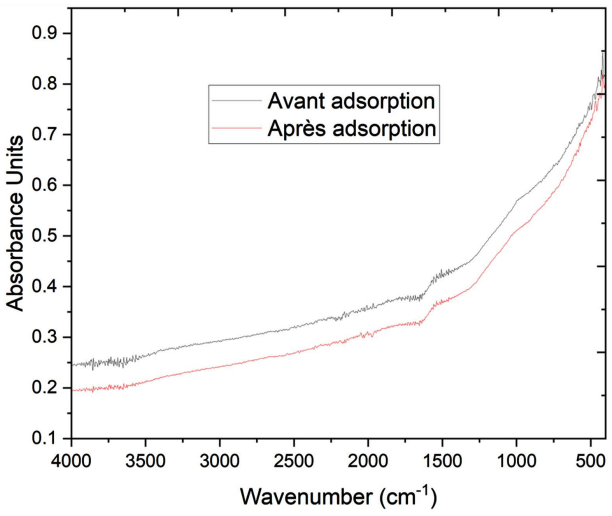

(b)

Figure 9. (a) FTIR spectra of CAP before and after adsorption of RC in aqueous solution; (b) FTIR spectra of CAK before and after adsorption of RC in aqueous solutions.

Figure 9 shows that the FTIR spectra of CAP and CAK before and after RC adsorption are identical. This indicates that the adsorption mechanism is dominated by physisorption.

3.9. Different Maximum Adsorption Capacity of RC on Other Adsorbents

Table 6 below shows the different capacities of RC on other adsorbents.

Table 6. Different maximum adsorption capacities of RC on other adsorbents.

Adsorbents	Adsorption capacity (mg/g)	References
Raw clay	27.03	[Ghribi *et al.*, 2014]
Coconut fiber residues	23.25	[21]
Raw cowpea pod	161.29	[Ayuba *et al.*, 2021]
Cattails	38.79	[Hu *et al.*, 2010]
Activated carbon	15.80	[22]
Activated carbon from asparagus bark activated with H_3PO_4	34.34	Present work
Activated carbon from asparagus bark activated with KOH	38.90	Present work

4. Conclusion

This work had a dual environmental impact: the recovery of organic waste through the preparation of activated carbon from the bark of the asparagus palm (*Laccosperma robustum*) and the decontamination of rivers through the adsorption of pollutants: RC red in aqueous solution using our activated carbon activated by chemical activation with phosphoric acid and potassium hydroxide. This study showed that the optimal adsorption conditions were 15 and 25 minutes for CAK and CAP agitation times, respectively, a mass of 0.05 g, and a pH = 2 for both ACs. The maximum adsorption quantities of RC were 34.338 mg/L for CAP and 38.901 mg/g for CAK for a concentration of 100 mg/L each. The Freundlich and Temkin isotherms best describe the RC adsorption process on activated carbons. The pseudo-first-order, pseudo-second-order, and Elovich kinetic models best describe the RC adsorption kinetics on CAP. Meanwhile, the pseudo-second-order and Elovich models best describe the RC adsorption kinetics on CAK. The results obtained showed that activated carbons are effective for the adsorption of effluents present in our rivers, such as the Congo River. These less expensive activated carbons may be an alternative solution for decision-makers in the context of environmental protection.

Conflicts of Interest

The authors declare no conflicts of interest regarding the publication of this paper.

References

[1] Mohamad Nor, N., Lau, L.C., Lee, K.T. and Mohamed, A.R. (2013) Synthesis of Activated Carbon from Lignocellulosic Biomass and Its Applications in Air Pollution Control—A Review. *Journal of Environmental Chemical Engineering*, **1**, 658-666.

https://doi.org/10.1016/j.jece.2013.09.017

[2] Laurent, A., Bakas, I., Clavreul, J., Bernstad, A., Niero, M., Gentil, E., *et al.* (2014) Review of LCA Studies of Solid Waste Management Systems—Part I: Lessons Learned and Perspectives. *Waste Management*, **34**, 573-588. https://doi.org/10.1016/j.wasman.2013.10.045

[3] https://www.medias241.com/Societe-acusee-de-pollution-a-Moanda-la-Comilog-se-met-ados-les-populations

[4] https://www.afrik21.africa/gabon-olam-palm-de-nouveau-accuse-de-pollution-environnementale-a-Ndende

[5] https://ejatlas.org/conflit/Pollution

[6] Ayuba, M.A. and Idoko, B. (2021) Adsorption of Congo Red Dye from Aqueous Solution Using Raw Cowpea (*Vigna unguiculata*) Husk. *Journal of Applied Surfaces and Interfaces*, **9**, 9-16.

[7] DEPA (Danish Environmental Protection Agency) (2000) Survey of Azo-Colorants in Denmark, Toxicity and Fate of Azo Dyes.

[8] Guiza, S. and Bagane, M. (2013) Étude cinétique de l'adsorption du rouge de Congo sur une bentonite. *Revue des sciences de l'eau*, **26**, 39-50. https://doi.org/10.7202/1014918ar

[9] Yakout, S.M. and Sharaf El-Deen, G. (2016) Characterization of Activated Carbon Prepared by Phosphoric Acid Activation of Olive Stones. *Arabian Journal of Chemistry*, **9**, S1155-S1162. https://doi.org/10.1016/j.arabjc.2011.12.002

[10] Langama, P.L.M., Anguile, J.J., Bissielou, C., Bouraïma, A., Ndong, A.N.M.M., Kouotou, D., *et al.* (2023) Preparation and Characterization of Activated Carbons from Asparagus Palm (*Laccosperma robustum*) Bark by Chemical Activation with H_3PO_4 and Koh. *American Journal of Analytical Chemistry*, **14**, 55-71. https://doi.org/10.4236/ajac.2023.142004

[11] Zhou, Y., Ge, L., Fan, N. and Xia, M. (2018) Adsorption of Congo Red from Aqueous Solution onto Shrimp Shell Powder. *Adsorption Science & Technology*, **36**, 1310-1330. https://doi.org/10.1177/0263617418768945

[12] Ghribi, A.A., Bagane, M.A. and Chlendi, M. (2014) Sorptive Removal of Congo Red from Aqueous Solutions Using Raw Clay: Batch and Dynamic Studies. *International Journal of Innovative Environmental Studies Research*, **2**, 45-56.

[13] Somasekhara Reddy, M.C., Sivaramakrishna, L. and Varada Reddy, A. (2012) The Use of an Agricultural Waste Material, Jujuba Seeds for the Removal of Anionic Dye (Congo Red) from Aqueous Medium. *Journal of Hazardous Materials*, **203**, 118-127. https://doi.org/10.1016/j.jhazmat.2011.11.083

[14] Litefti, K., Freire, M.S., Stitou, M. and González-Álvarez, J. (2019) Adsorption of an Anionic Dye (Congo Red) from Aqueous Solutions by Pine Bark. *Scientific Reports*, **9**, Article No. 16530. https://doi.org/10.1038/s41598-019-53046-z

[15] Aoulad, H.A.Y., N'diaye, D.A., Fahmi, D., Kankou, S.M. and Stitou, M. (2021) Adsorption of Congo Red from Aqueous Solution Using Typha Australis Leaves as a Low Cost Adsorbent. *Journal of Environmental Treatment Techniques*, **9**, 534-539.

[16] Naphtali Odogu, A., Daouda, K., Paul Keilah, L., Agbor Tabi, G., Ngouateu Rene, L., Julius Nsami, N., *et al.* (2020) Effect of Doping Activated Carbon Based *Ricinodendron heudelotti* Shells with AgNps on the Adsorption of Indigo Carmine and Its Antibacterial Properties. *Arabian Journal of Chemistry*, **13**, 5241-5253. https://doi.org/10.1016/j.arabjc.2020.03.002

[17] Lian, L., Guo, L. and Guo, C. (2009) Adsorption of Congo Red from Aqueous Solu-

tions onto Ca-Bentonite. *Journal of Hazardous Materials*, **161**, 126-131. https://doi.org/10.1016/j.jhazmat.2008.03.063

[18] Si, J., Yuan, T. and Cui, B. (2014) Exploring Strategies for Adsorption of Azo Dye Congo Red Using Free and Immobilized Biomasses of Trametes Pubescens. *Annals of Microbiology*, **65**, 411-421. https://doi.org/10.1007/s13213-014-0874-3

[19] Dawood, S. and Sen, T.K. (2012) Removal of Anionic Dye Congo Red from Aqueous Solution by Raw Pine and Acid-Treated Pine Cone Powder as Adsorbent: Equilibrium, Thermodynamic, Kinetics, Mechanism and Process Design. *Water Research*, **46**, 1933-1946. https://doi.org/10.1016/j.watres.2012.01.009

[20] Hu, Z., Chen, H., Ji, F. and Yuan, S. (2010) Removal of Congo Red from Aqueous Solution by Cattail Root. *Journal of Hazardous Materials*, **173**, 292-297. https://doi.org/10.1016/j.jhazmat.2009.08.082

[21] Rani, K.C., Naik, A., Chaurasiya, R.S. and Raghavarao, K.S.M.S. (2017) Removal of Toxic Congo Red Dye from Water Employing Low-Cost Coconut Residual Fiber. *Water Science and Technology*, **75**, 2225-2236. https://doi.org/10.2166/wst.2017.109

[22] Basava Rao, V.V. and Ram Mohan Rao, S. (2006) Adsorption Studies on Treatment of Textile Dyeing Industrial Effluent by Flyash. *Chemical Engineering Journal*, **116**, 77-84. https://doi.org/10.1016/j.cej.2005.09.029